FET-based integrated charge sensor for organ-on-chip applications

Aydogmus, H.; Dostanic, M.; Jahangiri, M.; Sinha, Rajarshi; Quiros Solano, W.F.; Mastrangeli, M.; Sarro, P.M.

DOI
10.1109/SENSORS47125.2020.9278692

Publication date
2020

Document Version
Final published version

Published in
IEEE Sensors, SENSORS 2020 - Conference Proceedings

FET-Based Integrated Charge Sensor for Organ-on-Chip Applications

Hande Aydogmus*, Milica Dostanić*, Mojtaba Jahangiri*, Rajarshi Sinha*,
William Fausto Quirós-Solano*†, Massimo Mastrangeli* and Pasqualina Maria Sarro*
*ECTM, Department of Microelectronics, TU Delft, The Netherlands
†BIOND Solutions BV, The Netherlands
Email: H.Aydogmus@tudelft.nl

***Abstract*—We present an extremely compact field effect transistor (FET)-based electrochemical sensor for *in situ* real-time and label-free measurement of ion concentrations in the cell culture area of organs-on-chip (OoCs) devices. This sensor replaces the functionality of an external reference electrode, crucial in standard electrochemical sensing, by controlling the FET threshold voltage via a capacitive control gate. The silicon- and polymer-based charge sensor can be integrated in OoC platforms by means of a wafer-scale and CMOS-compatible microfabrication process. This fabrication approach inherently allows a superior level of accuracy, repeatability and scalability compared to common OoC manufacturing methods. The sensor combines in a single device the complementary benefits of silicon-based electronics and of flexible polymer membranes with integrated microelectrodes – congenial substrates to sustain dynamic stimuli and mimic physiological tissue microenvironments. The integration of the polymer membrane in the sensing region makes this miniature sensor a preferable option for high sensitivity biochemical measurements in OoC applications, including monitoring the pH of cell culture media and of tissue culturing microenvironments, quantification of ion displacement in cells, and complementary research on disease modeling.**

I. Introduction

Living cells and tissues are constantly going through biochemical processes, and it is crucial to investigate in real-time how these processes are occurring for a thorough understanding. For example, neuronal signal transmission [1], vasodilation [2] or the tightness of the blood-brain-barrier [3] can all be evaluated by monitoring the production or concentration of ions. Electrochemical sensors can be employed to investigate these phenomena. Most of these sensors employ an external reference electrode to provide the reference potential and a working electrode where chemical reactions occur at close proximity. However, a major downside of using external reference electrodes, usually made from Ag/AgCl, is that, even though they are expected to have constant potentials, they can dissolve in the electrolyte over time, thus affecting the ion concentration and the electrochemical potential. If the volume of the solution is small, this problem becomes more significant and cannot be disregarded [4]. Moreover, these systems are bulky and difficult to implement into millimeter-sized devices where only few microliters of electrolyte are available to investigate reactions or chemical changes. An application of rising importance of such small functional devices is represented by organs-on-chips (OoCs).

OoCs are dynamic cell culture devices which recapitulate organ functions and mimic cell physiological environment to enhance the efficiency of drug development and disease modelling [5]. Monitoring cell conditions and microenvironment in real time is crucial to achieve the envisioned OoC functionality. However, most sensing in OoCs currently needs optical microscopy systems, which cannot monitor all relevant parameters at once, besides being bulky and costly. Hence real-time monitoring of biological cues without relying on optical systems is an unmet need for OoCs [6]. To provide compact sensing solutions in OoCs, we propose to use field effect transistor (FET)-based electrochemical sensors.

The first application of a FET for ion sensitive analysis goes back to the 1970s, where silicon-based fabrication techniques were used to analyse how the electrolyte in the environment was affecting the working point of the transistor. Lauks *et al.* [7] were among the first to implement extended gate electrodes with ion-selective membranes. Other examples include measuring neuron's action potential and metabolic activity [8], [9]; monitoring embryonic cardiac myocytes [10] and pH of the environment [11] by a flexible substrate. These FET-based sensors were still in need of an external and bulky reference electrode in order to set the working point of the transistor. Organic FET-based sensors were also employed as in the case of [12] and [13]. However, [12] was still in need of an external reference electrode to be used as the gate terminal and the electrical properties of silicon could be hardly reproduced by means of conductive polymers (*e.g.*, high voltages were needed to 'turn-on' the transistor, as in the case of [11], [13]).

Here, we present a floating-gate FET-based sensor to monitor the pH of the microenvironment and the well-being of biological cells in an OoC device. The device is fabricated on a hybrid silicon/polymer substrate featuring a polymer-based sensing area (Fig.1(a)-(c)). Instead of using an external reference electrode, the threshold voltage of the transistor is modulated by using a control gate capacitively coupled to an insulated floating gate. This approach is inspired by prior works in literature, such as [14]–[18]. In the modified and advanced device that we propose here, the silicon-based part contains all the electronics, including source and drain terminals of the transistor and pads of the gates. The polymer-based part consists of extended sensing electrodes suspended on a polydimethylsiloxane (PDMS) membrane. PDMS is used to

978-1-7281-6801-2/20/$31.00 ©2020 IEEE

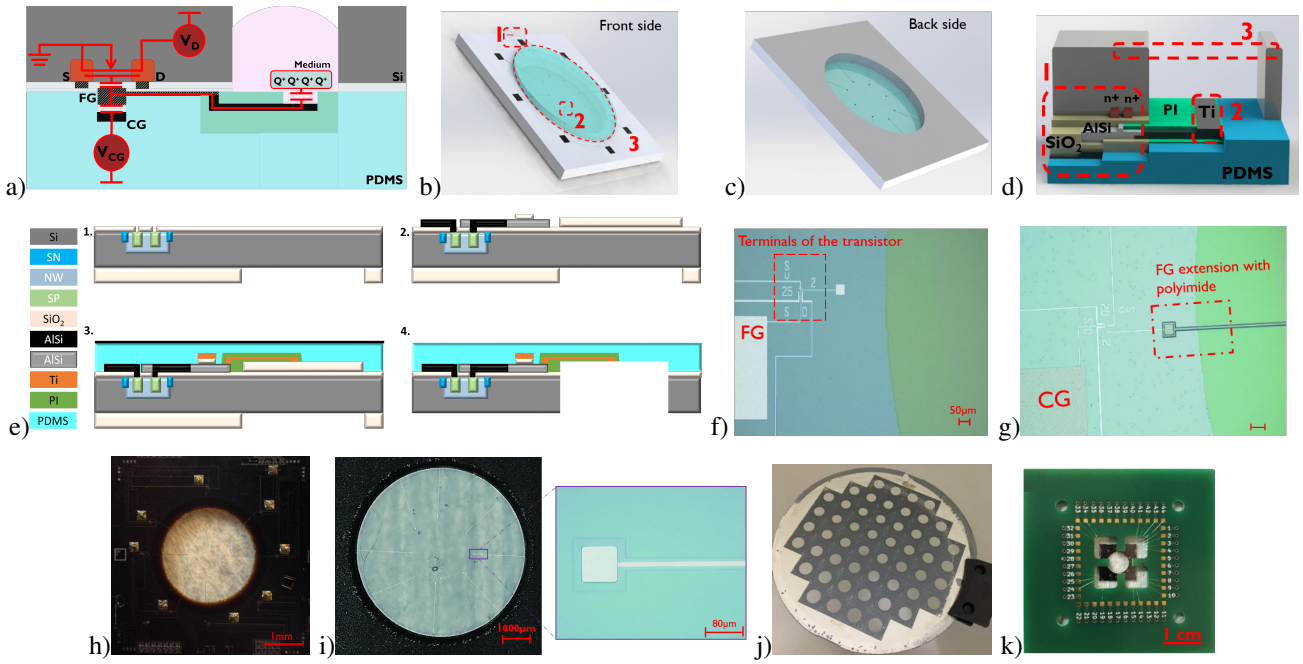

Fig. 1. The OoC-integrated FGFET-based charge sensor. a) Electrical schematic of the FGFET, evidencing the coupling of the control gate to the floating gate. b) Sketch of front and c) back side of a single chip. d) FGFET cross-section: (1) control and floating gates, (2) PI-encapsulated Ti gate extension on suspended PDMS membrane, (3) Si-etched well to host the solutions. (e) Fabrication flowchart of the sensor. Source terminal of the transistor is shown with lines for clarification. (f) Optical picture showing floating-gate, additional oxide on the membrane area and interconnects (scale bar: $50\mu m$). (g) Optical picture of PI-insulated gate extension (scale bar: $50\mu m$). (h) Front-side view of a single chip, showing 4 nMOS and 4 pMOS FETs and the suspended PDMS membrane with gate extensions. (i) Back-side view of a single chip (left), with close-up of a single gate extension on PDMS (right) with only the sensing area ($80\mu m$ x $80\mu m$) exposed to ions in the environment. j) 4-inch wafer-scale fabrication of the silicon/polymer-based OoCs with integrated charge sensors. k) A single chip glued and wire-bonded to a custom designed PCB to allow access to the sensing area during measurements.

form the sensing region as it provides cell-friendly biomechanical properties (compliance, elasticity, and biocompatibility) and it ensures optical access by its transparency. The extended electrodes are sandwiched between two polyimide (PI) layers, in order to insulate the electrodes and expose only a specific area to the solution-under-test (Fig. 1(d)). The fabrication process is fully CMOS compatible, and provides a soft and transparent substrate for the cells.

The working principle of the proposed device is based on the conservation of charges on the floating gate [14]–[17]. The control gate capacitively controls the floating gate and acts as reference electrode. In presence of an electrolyte at the sensing region, the additional charge which is in close proximity to the floating gate causes charge separation on the floating gate and modulates the charge carrier density of the transistor's channel. This in turn modulates the threshold voltage of the FET, which can be monitored by 1) tracking the value of the drain current (I_D) for a given input value of the control-gate voltage V_{CG}, or 2) tracking the I_D vs V_{GS} curve to extract the (shift in) threshold voltage itself.

II. Fabrication

A 4-inch, 525 μm-thick, single-side polished p-type silicon wafer was used for the fabrication of both nMOS- and pMOS-based sensors, partly based on a standard BiCMOS process (Fig.1(e)). N-Wells and source and drain terminals were defined by ion implantation, and 200 nm of gate oxide was thermally grown and lithographically patterned. A 6 μm-thick oxide layer was then deposited by plasma-enhanced chemical vapour deposition (PECVD) on the wafer backside to serve as hard mask for backside Si etching. Frontside contacts were opened to reach all terminals of the FETs (Fig.1(e):1).

The first metallization layer, consisting of interconnects and floating-gate pad without the extensions, used 600 nm of sputtered AlSi (Fig. 1(f)). 500 nm of additional PECVD oxide was deposited on the wafer frontside, in order to have a smooth landing during backside Si etching later used to release the PDMS membranes. A 50 nm-thick oxide was deposited as the dielectric layer between floating gate and the control gate. Vias were opened on the front side, before the polymer processing steps (Fig.1(e):2). Two layers of Polyimide (PI, from FUJIFILM) were deposited and patterned to sandwich the second metal layer. This was done for two reasons: 1) to introduce a stress-buffering transition layer between metal and PDMS (because of the intermediate mechanical properties of PI), and 2) to act as an electrical insulation layer (Fig. 1(g)). The second metal layer (Ti, 200 nm) was used to form the control-gate pad and floating-gate extensions. Only the sensing pads, located at the end of the extensions, were afterwards opened to the environment (Fig.1(h)). A 20 μm-thick layer of PDMS (10:1) was then spin-coated on the substrate activated by low-power oxygen plasma to enhance adhesion. The PDMS formed the membrane where the extended electrodes would be

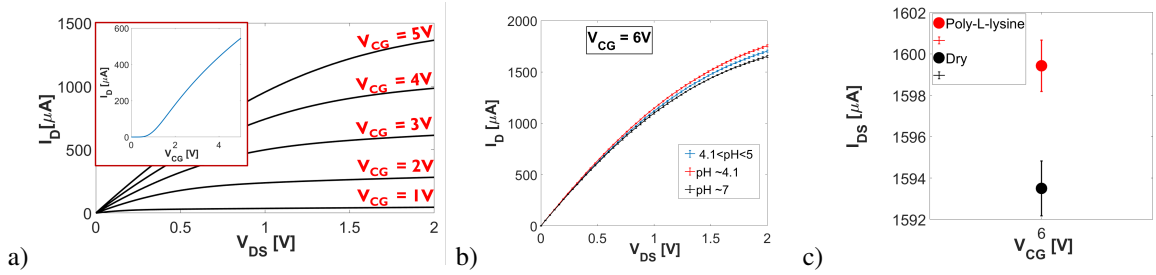

Fig. 2. Measured response for nMOS FET-based sensors. a) Characteristics of a single nMOS FET under dry conditions. b) nMOS output characteristics as function of solution pH. c) Mean and dispersion values of multiple sensor readings for a single nMOS-based sensor in dry state (black) and upon addition of a positively charged solution of poly-L-lysine ($250\frac{\mu g}{mL}$) at the sensing area (red).

TABLE I
MEAN AND VARIANCE OF THRESHOLD VOLTAGES (V_{TH}) FOR ALL FET TRANSISTORS FABRICATED IN A SINGLE FULL WAFER (4 PMOS AND 4 NMOS PER CHIP, 52 CHIPS IN TOTAL.)

V_{TH}	nMOS	pMOS
Average (V)	0.44	-3.69
Variance (V)	$7 \cdot 10^{-4}$	0.01

suspended and additionally served as the bottom of a well, later confined by the etched Si substrate, used to contain analytes and cell culture media. A 200 nm-thick AlSi layer was sputtered to act as hard mask for the upcoming etch steps (Fig.1(e):3). The Si substrate was finally etched from the backside with landing on the oxide layer as mentioned, and all masking layers were removed by wet etching (Fig. 1(e):4, (Fig.1(i)). By means of this process, we incorporated a well with the suspended sensing electrodes of 8 Si FET-based sensors on every chip.

Finally the processed wafer (Fig.1(j)) was saw-diced into 52 chips (size of 1 cm by 1 cm), which were assembled by gluing and wire bonding onto custom-designed PCBs to facilitate the ensuing measurements (Fig.1(k)).

III. RESULTS

After wire bonding, the transistors were electrically characterized using a Source-Measurement Unit (Semiconductor Parameter Analyzer). A 4-needle probe station was used to apply the necessary bias voltage to FG-FET terminals and retrieve drain current values. Full-wafer measurements of threshold voltages (Fig.2 (a)) without any liquid at the sensing area are summarized in Table I. Threshold voltages of transistors show relatively small variance. It is worth noting that the PCB was especially designed to simplify the access to the sensing area.

A. pH & Poly-L-Lysine Measurements

Since pH is an important variable to monitor the well-being of cells and their microenvironment, in this preliminary study the charge sensor was employed as a pH sensor. To do so, approximately 50 nm of silicon dioxide was left on top of the sensing area. This layer served as the functional surface, since H^+ ions can bond to the hydroxyl groups at the SiO_2 surface. DI water (pH $\approx$ 7), a commercially available solution with pH of 4.1 and its dilutions with DI water were used to characterize the response of the sensor. The diluted solutions was expected to have an intermediate pH value. Consecutive sensor readings where carried out to track the changes in response to the different pH levels. Fig.2(b) shows mean value and dispersion of multiple measurements for different pH values of the solutions. The consecutive sensor readings proved the real-time measurement ability and the stability of the sensor, suitable to track the pH changes in cell culture media. Additionally, we tested the sensor response to Poly-L-lysine (Sigma-Aldrich), a positively charged polymer frequently used for mammalian cell culturing applications [15] and which holds great therapeutic promise [19]. Preliminary real-time sensor measurements showed an increase in I_D upon introduction of the polymer to the dry sensing area, an important first step towards future cell culture experiments (Fig.2(c)).

IV. CONCLUSION

We have presented a novel and extremely compact FG-FET-based electrochemical sensor for OoC applications that does not need an external reference electrode. The unique feature of this sensor is that it combines the benefits of silicon-based technology and of flexible polymer membranes, the latter used as cell substrates in the OoC sensing area to mimic the physiological microenvironment of cells. Using silicon- and polymer-based microfabrication, 52 chips were obtained per wafer, each chip containing 4 nMOS and 4 pMOS transistors with similar characteristics, proving the reliability and scalability of the fabrication process. Promising preliminary measurements were performed with small concentrations of pH calibration liquids and aminoacid polymers, where we observed both the linear change in drain current due to proximal charges and the ability to work as biosensor for cell culturing microenvironments.

ACKNOWLEDGMENTS

The authors thank the staff at the Else Kooi Laboratory of TU Delft. This work was supported by the Netherlands Organ-on-Chip Initiative, an NWO gravitation project funded by the Ministry of Education, Culture and Science of the government of the Netherlands (024.003.001).

REFERENCES

[1] Hodgkin, A. L., & Huxley, A. F. (1952). A quantitative description of membrane current and its application to conduction and excitation in nerve. The Journal of physiology, 117(4), 500–544.

[2] Jackson, William F. (2000). Ion channels and vascular tone. Hypertension 35.1: 173-178.

[3] Hladky, S. B., & Barrand, M. A. (2016). Fluid and ion transfer across the blood–brain and blood–cerebrospinal fluid barriers; a comparative account of mechanisms and roles. Fluids and Barriers of the CNS, 13(1), 19.

[4] Shinwari, M. W. et. al., (2010). Microfabricated reference electrodes and their biosensing applications. Sensors, 10(3), 1679-1715.

[5] Marx, U., Andersson, T. B., Bahinski, A., Beilmann, M., Beken, S., Cassee, F. R., ...& Gaertner, C. (2016). Biology-inspired microphysiological system approaches to solve the prediction dilemma of substance testing. Altex, 33(3), 272.

[6] Mastrangeli, M., Millet, S., & van den Eijnden-van Raaij, J. (2019). Organ-on-chip in development: towards a roadmap for organs-on-chip.

[7] Spiegel, J. V., Lauks, I., Chan, P., & Babic, D. (1983). The extended gate chemically sensitive field effect transistor as multi-species microprobe. Sensors and Actuators, 4, 291-298.

[8] Fromherz, P., Offenhausser, A., Vetter, T., & Weis, J. (1991). A neuron-silicon junction: a Retzius cell of the leech on an insulated-gate field-effect transistor. Science, 252(5010), 1290-1293.

[9] Martinoia, S., Rosso, N., Grattarola, M., Lorenzelli, L., Margesin, B., & Zen, M. (2001). Development of ISFET array-based microsystems for bioelectrochemical measurements of cell populations. Biosensors and Bioelectronics, 16(9-12), 1043-1050.

[10] Ecken, H., Ingebrandt, S., Krause, M., Richter, D., Hara, M., & Offenhäusser, A. (2003). 64-Channel extended gate electrode arrays for extracellular signal recording. Electrochimica acta, 48(20-22), 3355-3362.

[11] Loi, A., Manunza, I., & Bonfiglio, A. (2005). Flexible, organic, ion-sensitive field-effect transistor. Applied Physics Letters, 86(10), 103512.

[12] Rivnay, J., Ramuz, M., Leleux, P., Hama, A., Huerta, M., & Owens, R. M. (2015). Organic electrochemical transistors for cell-based impedance sensing. Applied Physics Letters, 106(4), 8_1.

[13] Minamiki, T., Minami, T., Sasaki, Y., Wakida, S. I., Kurita, R., Niwa, O., & Tokito, S. (2016). Label-free detection of human glycoprotein (CgA) using an extended-gated organic transistor-based immunosensor. Sensors, 16(12), 2033.

[14] Barbaro, M., Bonfiglio, A., & Raffo, L. (2005). A charge-modulated FET for detection of biomolecular processes: conception, modeling, and simulation. IEEE Transactions on Electron Devices, 53(1), 158-166.

[15] Chen, B., Parashar, A., & Pandey, S. (2011). Folded floating-gate CMOS biosensor for the detection of charged biochemical molecules. IEEE Sensors Journal, 11(11), 2906-2910.

[16] Caboni, A., et al. "Organic-based sensor for chemical detection in aqueous solution." Applied Physics Letters 95.12 (2009): 253.

[17] Spanu, A., Lai, S., Cosseddu, P., Tedesco, M., Martinoia, S., & Bonfiglio, A. (2015). An organic transistor-based system for reference-less electrophysiological monitoring of excitable cells. Scientific reports, 5, 8807.

[18] Thomas, M. S., White, S. P., Dorfman, K. D., & Frisbie, C. D. (2018). Interfacial Charge Contributions to Chemical Sensing by Electrolyte-Gated Transistors with Floating Gates. The journal of physical chemistry letters, 9(6), 1335-1339.

[19] Orive, G., Tam, S. K., Pedraz, J. L., & Hallé, J. P. (2006). Biocompatibility of alginate–poly-l-lysine microcapsules for cell therapy. Biomaterials, 27(20), 3691-3700.